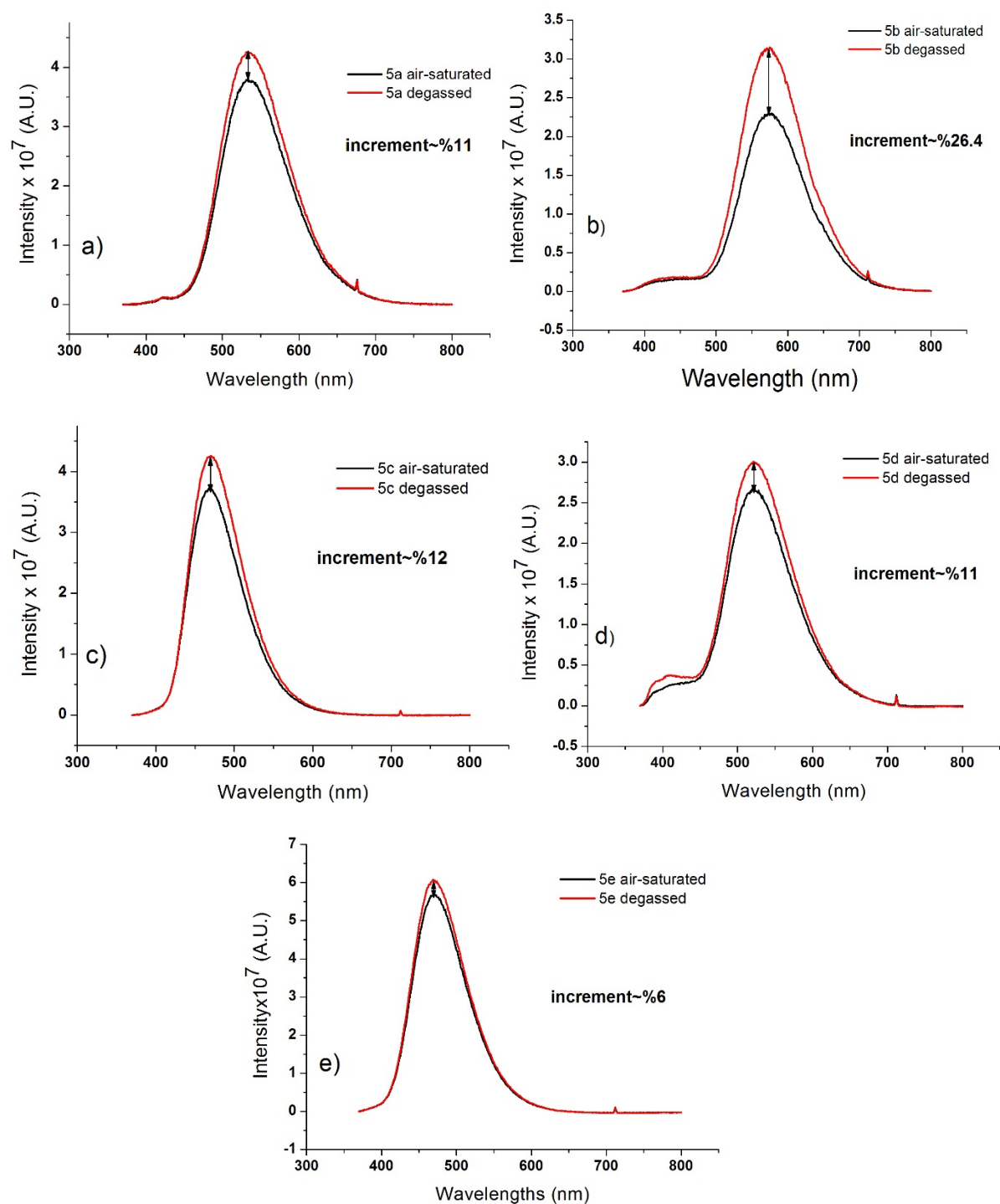
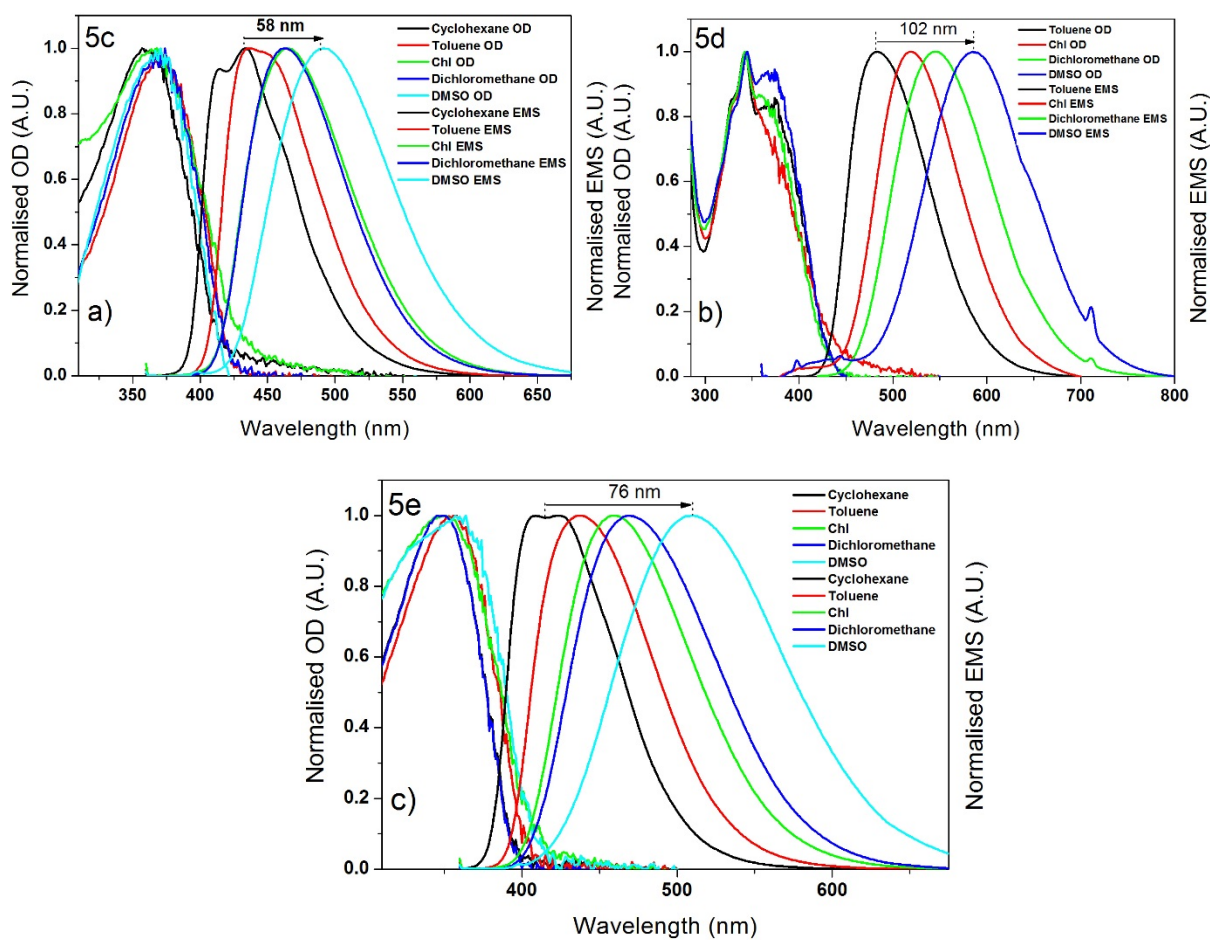


## Supplementary

### Steady-state measurements



**Figure 1** a) Steady-state spectra of molecules in air-saturated and degassed CHL solution a) 5a b) 5b c) 5c d) 5d e) 5e



**Figure 2** Absorption and photoluminescence spectra of materials in different polarity solvents  
 a) 5c b) 5d c) 5e

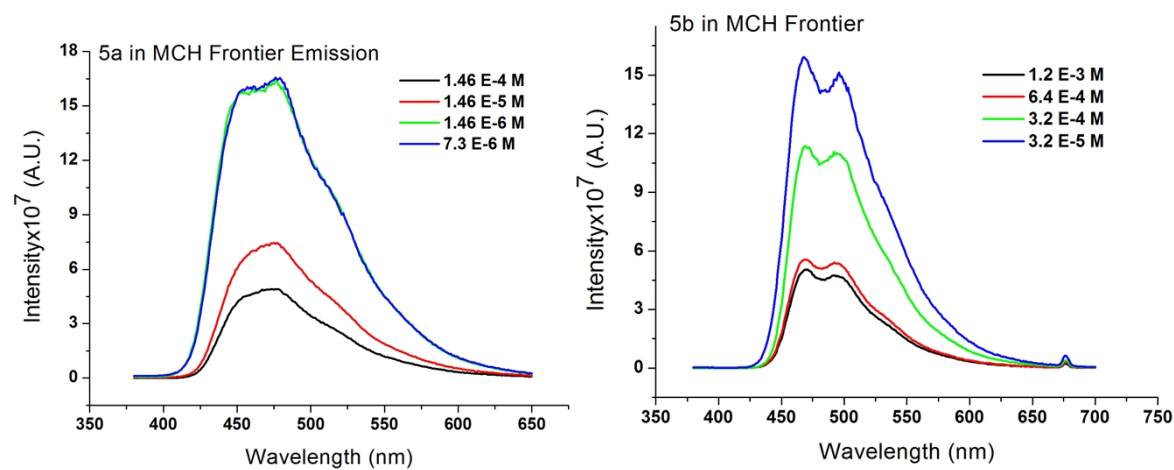
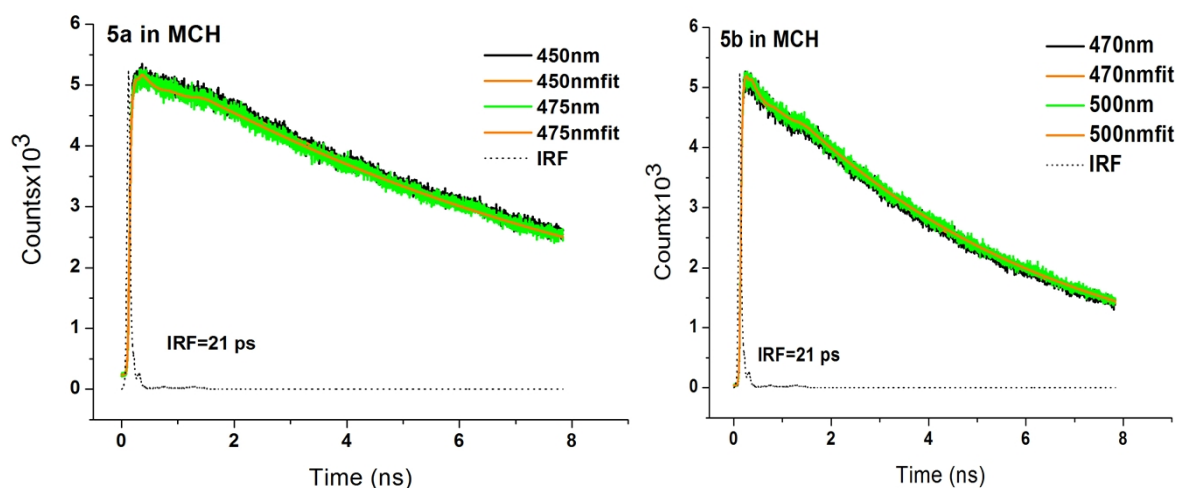


**Figure 3** The frontier emission are collected in different concentrations in MCH solution a) 5a  
 b) 5b



Materials in MCH	$\lambda_{ex}=368 \text{ nm}$	
	450 nm	475 nm
<b>5a</b>	$\tau_1=9.02 \text{ ns}$ $A1=0.18$ $\tau_2=0.094 \text{ ns}$ $A2=0.04$ $\chi= 1.1$	$\tau_1=8.98 \text{ ns}$ $A1=0.18$ $\tau_2=0.16 \text{ ns}$ $A2=0.028$ $\chi= 1.18$
<b>5b</b>	470 nm	500 nm
	$\tau_1=5.52 \text{ ns}$ $A1=0.24$ $\tau_2=0.13 \text{ ns}$ $A2=0.059$ $\chi= 1.1$	$\tau_1=5.57 \text{ ns}$ $A1=0.24$ $\tau_2=0.12 \text{ ns}$ $A2=0.065$ $\chi= 1.09$

**Figure 4** The fluorescence lifetime decays were collected by using single photon counting technique at different wavelength positions in degassed MCH solution at RT. Orange segmented lines are exponential fits. **a)** 5a **b)** 5b.

### 3. Synthesis and characterization

**3.1. General Details.** All reactions were carried out under nitrogen atmosphere. Solvent were distilled from appropriate reagents. The  $^1\text{H}$  and  $^{13}\text{C}$  spectra were recorded on a Bruker Spectrospin Avance DPX 500 spectroscopy operating at 500, 470 and 125 MHz, respectively. Mass spectra and High resolution Mass Spectra were recorded on Bruker Daltonics Microflex MALDI-TOF mass spectrometer and Bruker Daltonics micro TOF II ESI mass spectrometer, respectively. Cyclic voltammetry (CV) was performed in  $\text{CH}_2\text{Cl}_2$  containing 0.1 M

tetrabutylammonium perchlorate at room temperature using Gamry Instrument Reference 600. Platinum, platinum wire and Ag/AgCl were used as the working, counter and reference electrodes, respectively. Each oxidation potential was calibrated using ferrocene ( $E_{\text{ox}}^{1/2}=0.45$  V) as an external reference.

### Synthesis of **5a-e**:

#### 3,3'-(pyridine-2,6-diyl)bis(2-(4-bromophenyl)acrylonitrile) (**3**)

A solution of 2,6-Pyridinedicarboxaldehyde (**1**) (0,2 g, 1,48 mmol) and 4-Bromophenylacetonitrile (**2**) (0,527 g, 2,69 mmol) in absolute EtOH (10 ml) was treated with NaOH (32 mg, 0,8 mmol), which soluted in absolute EtOH (5 ml), portion wise and stirred at room temperature for 12 h. The precipitate was filtered and washed with cooled EtOH. The crude product was purified by crystallization (toluene) to afford (**3**) (0,49 g, 68%) as a white solid. m.p 185 °C.

FTIR (KBr),  $\nu$  [ $\text{cm}^{-1}$ ]: 3050, 2219, 2214, 1555, 1489, 832  $\text{cm}^{-1}$ ;

$^1\text{H-NMR}$  (500 MHz,  $\text{CDCl}_3$ ):  $\delta_{\text{H}}= 7,935$  (d, 2 H,  $J= 5$ ), 7,875 (t, 1 H,  $J= 7,5$ ), 7,63 (s, 2 H, CH=CCN), 7,555 (dd, 8 H,  $^2J= 5$   $^3J= 15$ ).  $^{13}\text{C-NMR}$  (125MHz,  $\text{CDCl}_3$ ):  $\delta= 155,21$ , 140,34, 138,04, 132,68, 132,40, 127,94, 124,50, 124,38, 116,84, 115,02. HRMS  $m/z$  calcd for  $\text{C}_{23}\text{H}_{14}\text{Br}_2\text{N}_3$ ; 489,9549  $[\text{M}+\text{H}]^+$ , found 489,9538  $[\text{M}+\text{H}]^+$

#### General procedure for synthesis of $\alpha,\beta$ -diarylacrylonitrile pyridines (**5a-e**)

To solution of **3** (1eq) in freshly distilled toluene:ethanol (30:10 ml) was added arylboronic acid (2,5 eq), 10% of arylboronic acid  $\text{Pd}(\text{PPh}_3)_4$  and  $\text{Na}_2\text{CO}_3$  (2M, aqueous, degassed 3 eq of arylboronic acid) were added sequentially. The mixture was stirred at reflux (110°C) for overnight under nitrogen. The solvent was evaporated and organic products were extracted into  $\text{CH}_2\text{Cl}_2$  (3x50 ml); the combined organic layers were dried ( $\text{Na}_2\text{SO}_4$ ) and concentrated under reduced pressure to obtain crude product which was subjected to silica-gel column chromatography to isolate isomeric mixture of product.

#### (2, *E*, *Z*, 2', *E*, *Z*)-3,3'-(pyridine-2,6-diyl)bis(2-(4-(anthracen-9-yl)phenyl)acrylonitrile) (**5a**)

**5a** was purified by a column chromatography on silica-gel using dichloromethane/hexane (1:1) as an eluent. Further purification of **5a** was recrystallized with chloroform to yield compound as a yellow solid (0.155 g, 55%); m.p. 262 °C.

FTIR (KBr),  $\nu$  [ $\text{cm}^{-1}$ ]: 3045, 2216, 1622, 1556, 1443, 1163, 822  $\text{cm}^{-1}$

<sup>1</sup>H-NMR (500 MHz, CDCl<sub>3</sub>): δ<sub>H</sub>= 8,47 (s, 2H), 8,08 (d, 2H, , *J*= 10), 8,02-7,95 (m, 9H), 7,90 (s, 2H), 7,61 (d, 4H, , *J*= 10), 7,525 (d, 4H, *J*= 5), 7,44-7,41 (m, 4H), 7,35-7,32 (m, 4H)

<sup>13</sup>C-NMR (125MHz, CDCl<sub>3</sub>): δ= 152,51, 140,98, 137,94, 135,53, 133,12, 132,19, 131,32, 130,03, 128,47, 126,58, 126,42, 125,73, 125,23, 124,29, 117,38, 115,78

HRMS *m/z* calcd for C<sub>51</sub>H<sub>32</sub>N<sub>3</sub>; 686,2590 [M+H]<sup>+</sup>, found 686,2589 [M+H]<sup>+</sup>

(2, *E*, *Z*, 2', *E*, *Z*)-3,3'-(pyridine-2,6-diyl)bis(2-(4'-(diphenylamino)-[1,1'-biphenyl]-4-yl)acrylonitrile) (**5b**)

**5b** was purified by a column chromatography on silica-gel using dichloromethane/hexane (1:1) as an eluent to yield compound as an orange solid (0.23 g, 50 %); m.p. 215 °C.

FTIR (KBr), ν [cm<sup>-1</sup>]: 3031, 2215, 1589, 1557, 1450, 1277, 819 cm<sup>-1</sup>

<sup>1</sup>H-NMR (500 MHz, CDCl<sub>3</sub>): δ<sub>H</sub>= 8,00 (d, 2H, *J*= 5), 7,89 (t, 1H, *J*= 10), 7,77 (d, 4H, *J*= 10), 7,73 (s, 2H), 7,61 (d, 4H, *J*= 10), 7,445 (d, 4H, *J*= 5), 7,23-7,20 (m, 8H), 7,08 (d, 12H, *J*= 10), 7,00-6,97 (m, 4H)

<sup>13</sup>C-NMR (125MHz, CDCl<sub>3</sub>): δ=147,99, 147,42, 133,01, 129,47, 127,95, 127,17, 127,09, 124,78, 124,13, 123,98, 123,42, 123,32, 117,06

HRMS *m/z* calcd for C<sub>59</sub>H<sub>42</sub>N<sub>5</sub>; 820,3434 [M+H]<sup>+</sup>, found 820,3476 [M+H]<sup>+</sup>

(2, *E*, *Z*, 2', *E*, *Z*)-3,3'-(pyridine-2,6-diyl)bis(2-(4-(thiophen-2-yl)phenyl)acrylonitrile) (**5c**)

**5c** was purified by a column chromatography on silica-gel using dichloromethane/hexane (1:2) as an eluent to yield compound as a light yellow solid (0.25 g, 70 %); m.p. 196 °C. FTIR (KBr), ν [cm<sup>-1</sup>]: 3063, 2217, 1669, 1553, 1425, 1157, 837, 822 cm<sup>-1</sup>

<sup>1</sup>H-NMR (500 MHz, CDCl<sub>3</sub>): δ<sub>H</sub>= 7,965 (d, 2H, *J*= 5), 7,87 (t, 1H, *J*= 10), 7,72 (d, 4H, *J*= 10), 7,68 (s, 2H), 7,64 (d, 4H, *J*= 10), 7,335 (d, 2H, *J*= 5), 7,275 (d, 2H, *J*= 5), 7,047 (dd, 2 H, <sup>2</sup>*J*= 1,5 <sup>3</sup>*J*= 5)

<sup>13</sup>C-NMR (125MHz, CDCl<sub>3</sub>): δ= 152,45, 143,05, 139,49, 137,89, 136,11, 132,61, 128,37, 127,03, 126,35, 125,90, 124,07, 117,12, 115,42

HRMS *m/z* calcd for C<sub>31</sub>H<sub>20</sub>N<sub>3</sub>S<sub>2</sub>; 498,1093 [M+H]<sup>+</sup>, found 498,1100 [M+H]<sup>+</sup>

(2, *E*, *Z*, 2', *E*, *Z*)-3,3'-(pyridine-2,6-diyl)bis(2-(4-(pyren-2-yl)phenyl)acrylonitrile) (**5d**)

**5d** was purified by recrystallization with dichloromethane and filtered then again recrystallization with toluene to yield compound as a dark orange solid (0,35 g, 67 %); m.p. 220 °C.

FTIR (KBr), ν [cm<sup>-1</sup>]: 3036, 2216, 1559, 1455, 846 cm<sup>-1</sup>

<sup>1</sup>H-NMR (500 MHz, CDCl<sub>3</sub>): δ<sub>H</sub>= 8,19-8,15 (m, 4H), 8,125 (d, 4H, *J*= 5), 8,05 (s, 4H), 8,01 (d, 4H, *J*= 10), 8,00-7,89 (m, 9H), 7,82 (s, 2H), 7,71(d, 4H, *J*= 10)

<sup>13</sup>C-NMR (125MHz, CDCl<sub>3</sub>): δ= 152,49, 143,17, 140,11, 137,88, 136,27, 132,76, 131,47, 131,39, 130,99, 130,94, 129,04, 128,45, 128,25, 127,91, 127,76, 127,41, 127,39, 126,56, 126,16, 125,37, 125,30, 125,08, 125,00, 124,85, 124,74, 124,20, 117,34, 115,66

HRMS *m/z* calcd for C<sub>55</sub>H<sub>32</sub>N<sub>3</sub>; 734,2590 [M+H]<sup>+</sup>, found 734,2568 [M+H]<sup>+</sup>

(2, *E*, *Z*, 2', *E*, *Z*)-3,3'-(pyridine-2,6-diyl)bis(2-(4-(naphthalen-1-yl)phenyl)acrylonitrile) (**5e**)

**5e** was purified by a column chromatography on silica-gel using dichloromethane/chloroform/hexane (1:1:2) as an eluent. Further purification of **5e** was recrystallized with chloroform to yield compound as a yellow solid to yield compound as a pale solid (0.22 g, 77 %); m.p. 218 °C.

FTIR (KBr), ν [cm<sup>-1</sup>]: 3038, 2219, 1560, 1456, 844, 788 cm<sup>-1</sup>

<sup>1</sup>H-NMR (500 MHz, CDCl<sub>3</sub>): δ<sub>H</sub>= 7,995 (d, 2H, *J*= 5), 7,91 (t, 1H, *J*= 10), 7,87-7,82 (m, 10H), 7,76 (s, 2H), 7,56 (d, 4H, *J*= 10), 7,50-7,42 (m, 5H), 7,39 (t, 3H, *J*= 5)

<sup>13</sup>C-NMR (125MHz, CDCl<sub>3</sub>): δ= 151,49, 141,69, 139,02, 137,94, 136,90, 132,80, 131,73, 130,30, 129,84, 127,40, 127,20, 125,96, 125,43, 125,35, 124,97, 124,64, 124,37, 123,17, 116,29, 114,65

HRMS *m/z* calcd for C<sub>43</sub>H<sub>28</sub>N<sub>3</sub>; 586,2278 [M+H]<sup>+</sup>, found 586,2264 [M+H]<sup>+</sup>

### 3.4. Electrochemical properties:

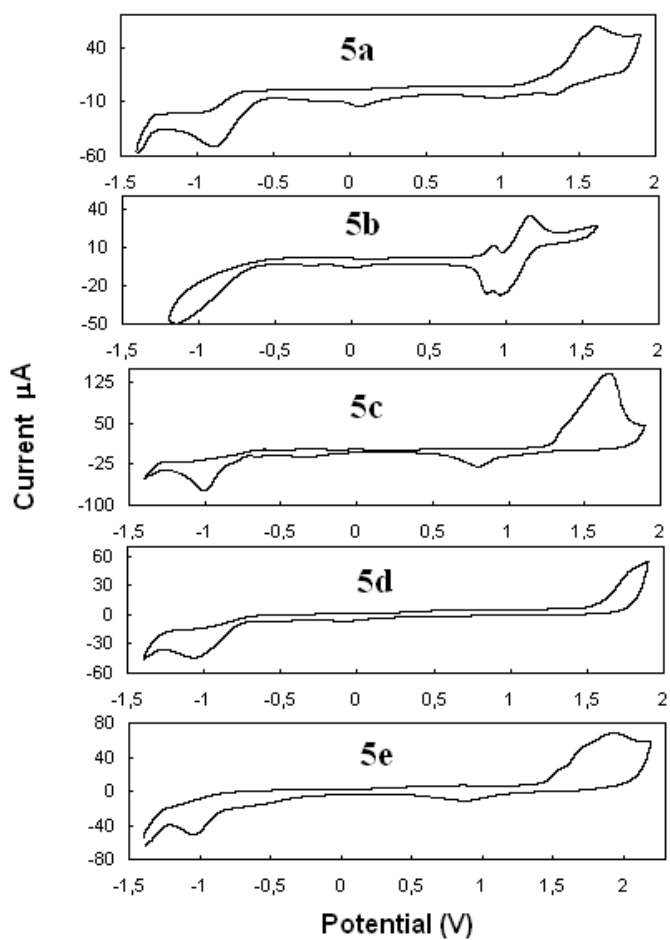
Electrochemical properties of **5a-e** were investigated by cyclic voltammetry. Cyclic voltammetry was performed in CH<sub>2</sub>Cl<sub>2</sub> containing 0.1 M tetrabutylammonium perchlorate at room temperature. All scans are shown in Fig.3. The electrochemical properties of these materials are listed in Table 2. **5a**, **5c**, **5d** and **5e** showed irreversible oxidation processes in the range between 1.05 and 1.55 V, whereas **5d** was reversible (0.83 V) due to the presence of anthracene groups. The HOMO (highest occupied molecular orbital) energy levels were calculated from oxidation potential using ferrocene as a standard referenced to the energy level of ferrocene (4.8 eV below the vacuum level) [3] and the LUMO (lowest unoccupied molecular orbital) levels were estimated by subtracting the band-gap energy (calculated from the extrapolation of the long wavelength) from the HOMO level.

The HOMO energy levels were obtained as -5.18, -5.40, -5.61, -5.75, and -5.90 eV for **5a-e**, respectively. The HOMO energy levels of (2, *E*, *Z*, 2', *E*, *Z*)-3,3'-(pyridine-2,6-diyl)bis(2-(4-

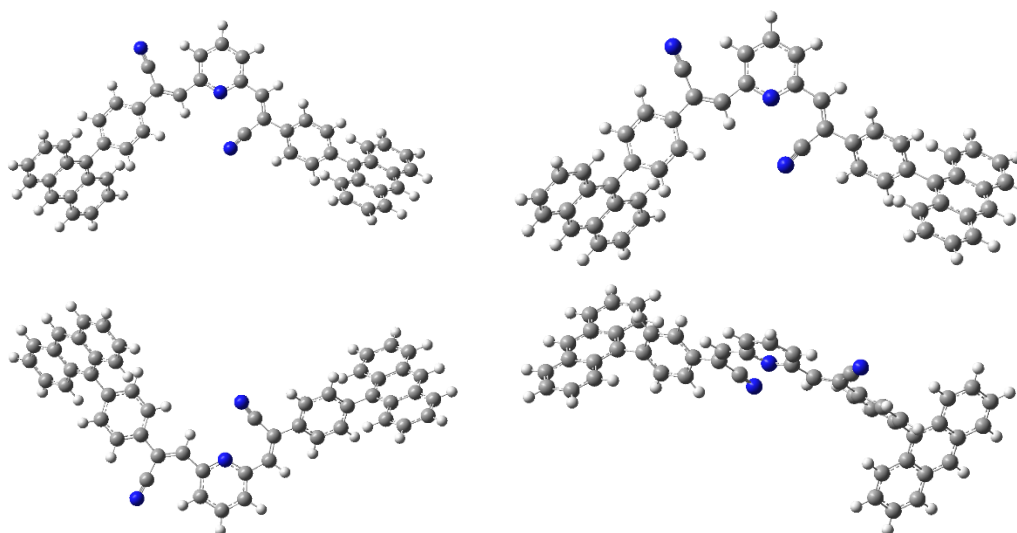
(anthracen-9-yl)phenyl)acrylonitrile, **5a**), (2, *E*, *Z*, 2', *E*, *Z*)-3,3'-(pyridine-2,6-diyl)bis(2-(4'-(diphenylamino)-[1,1'-biphenyl]-4-yl)acrylonitrile, **5b**) (2, *E*, *Z*, 2', *E*, *Z*)-3,3'-(pyridine-2,6-diyl)bis(2-(4-(thiophen-2-yl)phenyl)acrylonitrile, **5c**) and (2, *E*, *Z*, 2', *E*, *Z*)-3,3'-(pyridine-2,6-diyl)bis(2-(4-(pyren-2-yl)phenyl)acrylonitrile, **5d**) derivatives are slightly higher than 2-methyl-9,10-di(2-naphtyl)anthracene (MADN, -5.5 eV) and 9,10-di(2-naphtyl)anthracene (ADN, -5.8 eV).

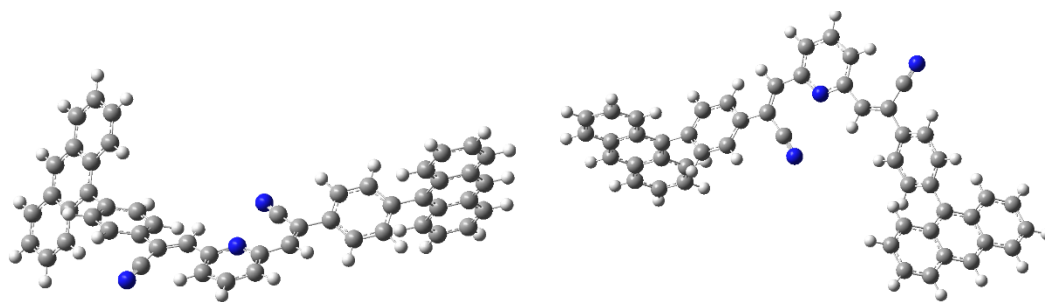
The initial geometry optimizations of all the structures leading to energy minima were achieved by using MM2 method followed by semi-empirical PM3 self-consistent fields molecular orbital (SCF MO) method [4,5] at the restricted level [6]. Then, geometry optimizations were achieved within the density functional theory (DFT, B3LYP) [7,8] at the level of (B3LYP/6-31G(d)) (restricted closed-shell). The exchange term of B3LYP consists of hybrid Hartree–Fock and local spin density (LSD) exchange functions with Becke's gradient correlation to LSD exchange [9]. The correlation term of B3LYP consists of the Vosko, Wilk, Nusair (VWN3) local correlation functional [10] and Lee, Yang, Parr (LYP) correlation correction functional. After B3LYP/6-31G(d) level of calculations, single point calculations at B3LYP/6-311+G(d,p) level were performed to obtain accurate frontier molecular orbital energy values. All the bond lengths were thoroughly searched in order to find out whether any bond cleavage occurred or not during the geometry optimization process. All these computations were performed by using Gaussian 09 package program [11]. Computational issues were discussed in more detail in the relevant section.

The geometry optimized structures of 5a and 5b at B3LYP/6-31G(d) level are shown in Figure X. In 5a, anthracene ring was found to be perpendicular to phenyl ring (interruption of  $\pi$ -conjugation within the molecule). Directions of the nitrile groups in 5a and 5b are opposite sides due to some possible intra molecular interactions (2.52Å CN...H, 3.3152Å CN...H noncovalant bond distances). It is clear from the geometry optimized structures that conjugation in 5b is better than the conjugation in 5a. Relatively better extension of conjugation in 5b causes decreasing energy gap between HOMO and LUMO (See Table X). On the other hand, computed and experimental frontier orbital energies of 5b are higher than the same orbitals in 5a (the sign of energy values should be kept in mind), this should be effect of electron donating ability of triphenylamine units. Considering experimental and computed  $E_g^{\text{opt}}$  values, the results show satisfactory parallelism.

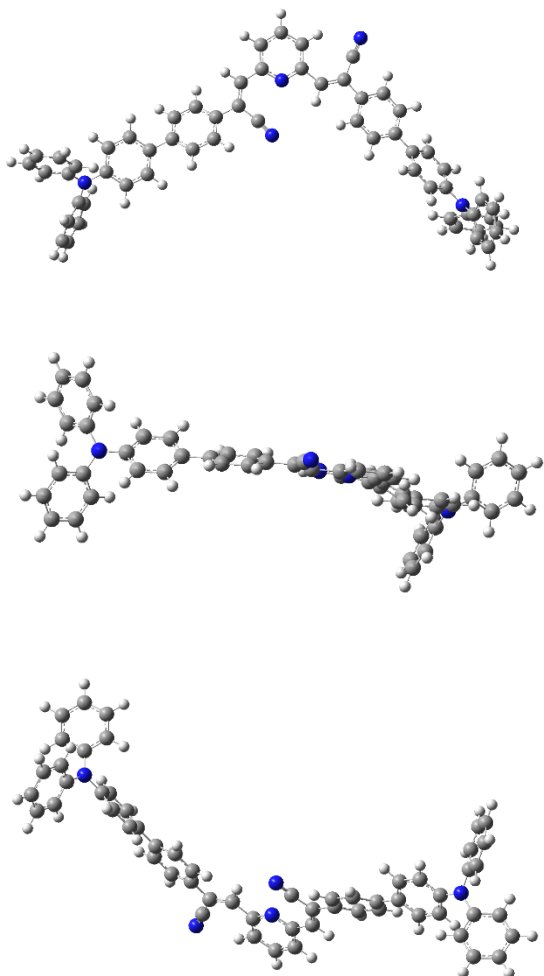


5a: B3LYP/6-31G(d) optimized structures with different orientations are shown.

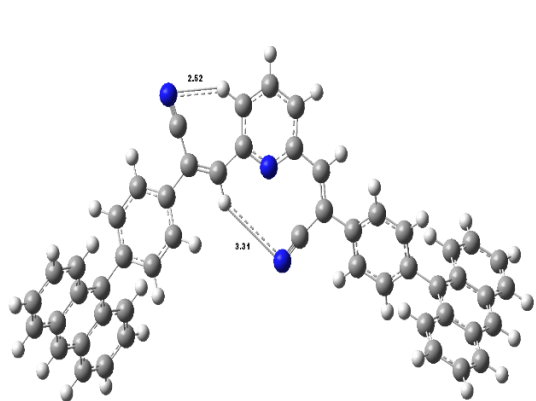




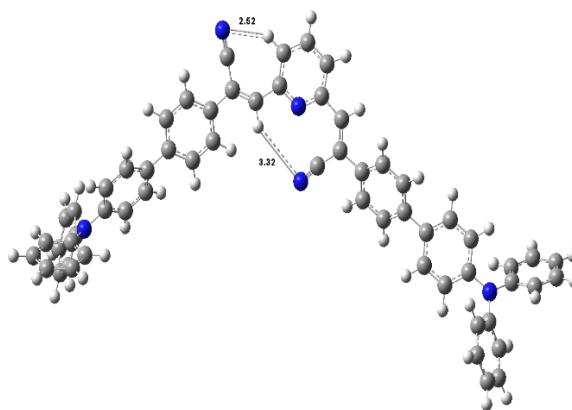
5b: B3LYP/6-31G(d) optimized structures with different orientations are shown.



Computed possible Hydrogen Bond (or *intra-molecular bond*) Lengths (in Å).

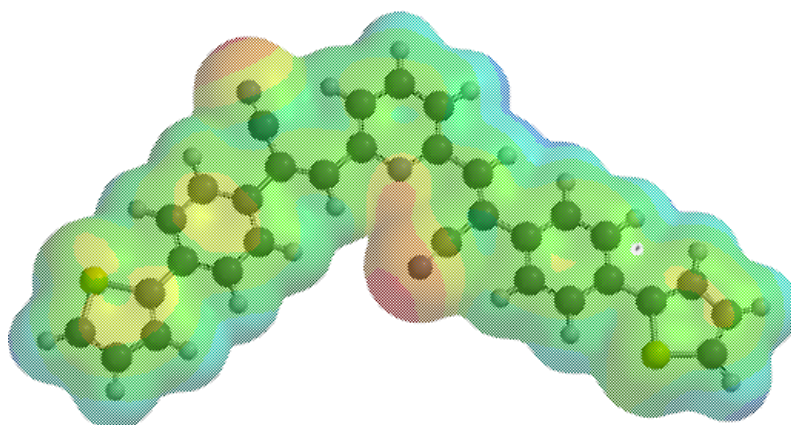


5a

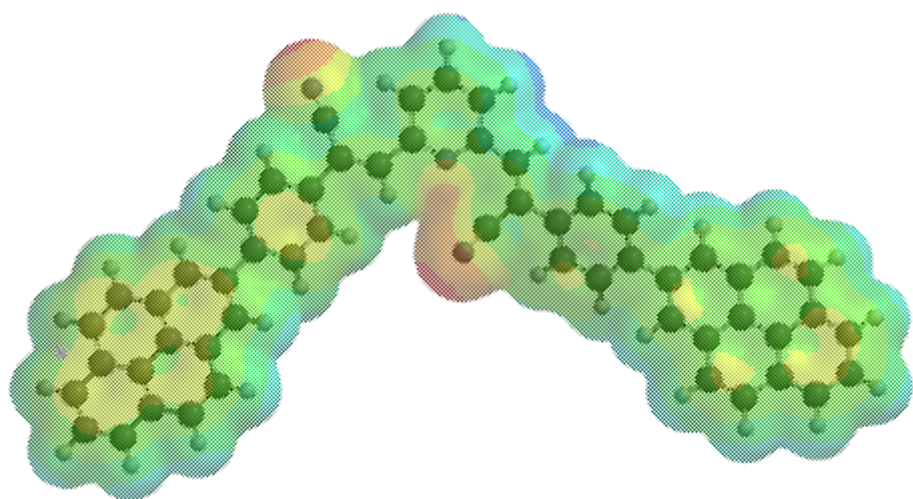


5b

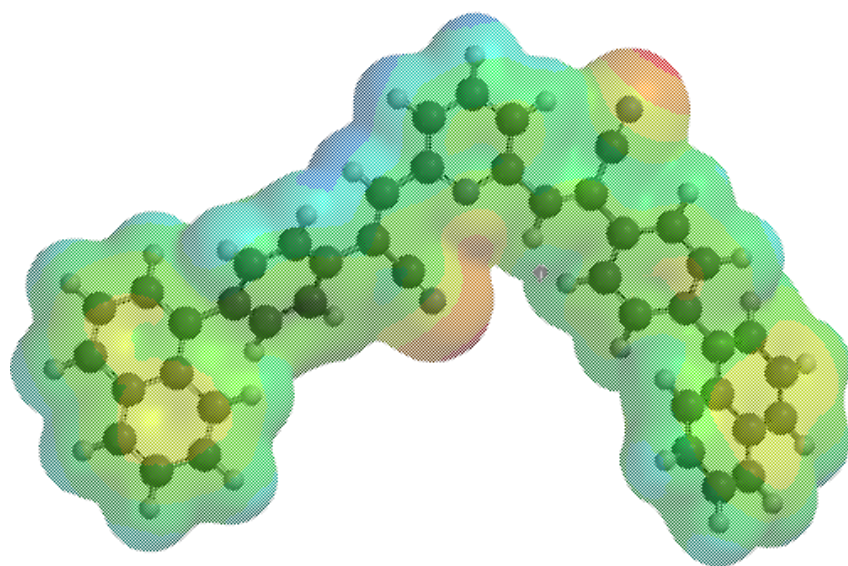
The charge distribution graphs of 5 c.d.e



5c



5d



**References**

- [1] M.Hanack, B. Behnisch, H.Häckl, P. Martinez-Ruiz, K.-H. Schweikart, Influence of the cyano-group on the optical properties of oligomeric PPV-derivatives, *Thin Solid Films*, 417, 26-31, **2002**
- [2] Stephen A. DiBiase, Bruce A. Lipisko, Anthony Haag, Raymond A. Wolak and George W. Gokel, Direct synthesis of  $\alpha,\beta$ -Unsaturated nitriles from acetonitrile and carbonyl compounds: survey, crown effects and experimental conditons, *J.Org.Chem.*, 44, 25, 4640-4649, 1979
- [3] Ibrahim M.A, Roth H.K., Zhokhavets U, Gobsch G, Sensfuss S., Flexible large area polymer solar cells based on poly(3-hexylthiophene)/fullerene, *Solar Energy Mat. and Solar Cells* 85 (2005),13-20
- [4] J.J.P. Stewart, Optimization of parameters for semi empirical methods I, *Method J. Comput. Chem.* 10, 209–220, **1989**.
- [5] J.J.P. Stewart, Optimization of parameters for semi empirical methods II, *Appl. Comput. Chem.* 10, 221–264, **1989**.
- [6] A.R. Leach, *Molecular Modeling*, Longman, Essex, **1997**.
- [7] W. Kohn, L.J. Sham, Self-consistent equations including exchange and correlation effects, *Phys. Rev.* 140, 1133–1138, **1965**.
- [8] R.G. Parr, W. Yang, *Density Functional Theory of Atoms and Molecules*, Oxford University Press, London, **1989**.
- [9] A.D. Becke, Density-functional exchange-energy approximation with correct asymptotic behavior, *Phys. Rev. A* 38, 3098–3100, **1988**.
- [10] S.H. Vosko, L. Vilk, M. Nusair, Accurate spin-dependent electron liquid correlation energies for local spin density calculations: a critical analysis, *Can. J. Phys.* 58, 1200–1211, **1980**.
- [11] M.F. Frisch, G.W. Trucks, H.B. Schlegel, G.E. Scuseria, M.A. Robb, J.R. Cheesman, et al., *Gaussian 09*, Gaussian Inc., Pittsburg, PA, **2009**.



